Environmental Science Processes & Impacts

ROYAL SOCIETY OF CHEMISTRY

PAPER

View Article Online
View Journal | View Issue

Cite this: *Environ. Sci.: Processes Impacts*, 2024, **26**, 2227

Leachability of per- and poly-fluoroalkyl substances from contaminated concrete†

Prashant Srivastava, *[a] Grant Douglas, [b] Greg B. Davis, [b] Rai S. Kookana, [a] Canh Tien Trinh Nguyen, [a] Mike Williams, [a] Karl Bowles [cd] and Jason K. Kirby [a]

The historical use and storage of aqueous film-forming foams (AFFF) containing per- and poly-fluoroalkyl substances (PFAS) at a range of sites including airports, defence, and port facilities have resulted in a legacy of contaminated infrastructure such as concrete. Contaminated concrete constitutes an ongoing source of PFAS contamination requiring management to ensure the protection of human health and the environment. In this study, modified Leaching Environmental Assessment Framework (LEAF) and Australian Standard Leaching Procedure (ASLP) were used to examine the leachability of PFAS, specifically, perfluorooctanesulfonate (PFOS), perfluorooctanoic acid (PFOA), perfluorohexanesulfonate (PFHxS) and perfluorohexanoic acid (PFHxA) from AFFF-contaminated concrete collected from an Australian Defence Fire Training Area (FTA). In general, PFAS readily leached from intact contaminated concrete monoliths with the cumulative proportion (%) decreasing in the order: PFHxA (>95%) > PFOS (26–84%) ≈ PFHxS (14–78%) > PFOA (<1–54%). Higher leachability for PFHxA from concrete is consistent with previous findings for solids, however, inconsistent for PFOA with higher retention (lower leachability) in concrete as compared to PFOS. Duration of exposure to water (0.5–48 h) and temperature (25 °C and 50 °C) had little influence on the proportion of PFAS leachability from powdered concrete. A higher proportion of PFAS leached from a <2 mm concrete powder size fraction as compared to 2–20 mm and 20 mm size fractions. This behavior reflects an increase in surface area with decreasing concrete particle size. Reducing the particle size could enhance PFAS removal from waste concrete.

Received 14th August 2024
Accepted 26th October 2024

DOI: 10.1039/d4em00482e

rsc.li/espi

Environmental significance

This research reveals significant PFAS leachability from impacted concrete and emphasizes the need to effectively manage PFAS-impacted concrete infrastructure at contaminated sites. Further research is required to develop and validate leaching tests under field conditions to accurately assess PFAS leaching behavior in concrete and inform remediation strategies.

Introduction

Per- and poly-fluoroalkyl substances (PFAS) are a diverse group of synthetic compounds that have been widely applied in industrial and consumer product applications since the 1950s[1–3] following the development of poly(tetrafluoroethylene) in 1938.[4] Aqueous film-forming foam (AFFF) products containing PFAS have been used worldwide, including in Australia, since the 1970s to suppress flammable liquid fires (https://www.pfas.gov.au/about-pfas). Since the early 2000s, industries and authorities have commenced phasing out AFFF and replacing it with non-PFAS options. The Australian Department of Defence began transitioning from foams containing PFOS in 2004, and in 2021 transitioned all aviation rescue firefighting vehicles to PFAS-free foams.[5]

The persistence and high mobility of PFAS at sites from historical AFFF usage have resulted in their widespread environmental distribution and concerns for human exposure and health.[6,7] The Australian Department of Health recommends that as a precaution, ongoing human exposure should be minimized.[8]

The historical use of AFFF containing perfluorooctanesulfonate (PFOS) and perfluorooctanoic acid (PFOA) at airports and Defence sites was often associated with fire suppression activities at fire

[a]*Commonwealth Scientific and Industrial Research Organization, Environment Research Unit, Industry Environments Program, Waite Campus, Urrbrae, SA 5064, Australia. E-mail: Prashant.Srivastava@csiro.au*

[b]*Commonwealth Scientific and Industrial Research Organization, Environment Research Unit, Industry Environments Program, 7 Conlon St., Waterford, WA 6152, Australia*

[c]*Jacobs, L7/177 Pacific Hwy, North Sydney, 2060, Australia*

[d]*Queensland Alliance for Environmental Health Sciences (QAEHS), The University of Queensland, Cornwall Street, Woolloongabba, QLD, 4102, Australia*

† Electronic supplementary information (ESI) available. See DOI: https://doi.org/10.1039/d4em00482e

training areas (FTA), airport taxiways, runways, and hangars.[9] This use of AFFF at the time has resulted in PFAS contamination of not only the environment (*e.g.*, soils, surface waters, and groundwater) but also infrastructure associated with firefighting activities (*e.g.*, asphalt runways and hangers, and concrete pads and drains). Extensive research has been undertaken into understanding the fate, behavior, and effects of PFAS in the environment;[10–13] however, little research to date has focused on PFAS-contaminated infrastructure, such as concrete and asphalt.[9] The spatial (horizontal and vertical) distribution of PFAS in concrete pads and drains at airports has been highlighted.[9,14–17] Contaminated concrete has the potential to be an ongoing source of PFAS contamination through leaching and wash-off, for example, during rainfall events, and firefighting training activities into surface soils and waters, and transported into subsurface soils and groundwaters.[14,15] Increasingly, managers of PFAS-contaminated sites (*e.g.*, airports) are looking for short- and long-term mitigation and management options (*in situ* and *ex situ*) for PFAS-contaminated concrete that can often be present in large volumes and have complex PFAS mixtures reflecting the use of different generations of AFFF, and variable concentrations.[9,17,18]

The leaching behavior and waste classification of contaminants (*e.g.*, PFAS) in soils and solids are commonly assessed using standard leaching tests such as the United States Environmental Protection Agency (US EPA) Leaching Environmental Assessment Framework (LEAF)[19–22] and the Australian Standard Leaching Procedure (ASLP).[23] The US EPA LEAF consists of four methods (LEAF 1313 to 1316) commonly used as an evaluation system to assess the leachability of contaminants of concern from a wide range of granular or solid materials.[19–22] The ASLP is commonly used for contaminated soil or hazardous waste classification and has been applied to assess the maximum leaching potential of PFAS in solids.[24,25] Recently the methods have been used to assess PFAS stabilization strategies for soils[26] and to evaluate alternate methods for mimicking natural leaching in soils.[27] In this study, modified LEAF 1313 and 1315, and ASLP standard tests were used to examine the leachability of four PFAS – three long-chain PFAS: PFOS, PFOA and perfluorohexanesulfonate (PFHxS), and a short-chain PFAS: perfluorohexanoic acid (PFHxA) – from AFFF-contaminated concrete collected from an Australian Defence FTA. The findings were used to inform mitigation and management decisions including treatment, disposal, and repurposing for PFAS-contaminated concrete at FTAs across Australia but are equally useful internationally.

Materials and methods

Chemicals and standards

Four native and isotopically labelled PFAS (PFOS linear, PFOA, PFHxS and PFHxA) standards were procured from Wellington Laboratories (Canada). The native and isotopically labelled PFAS stock solutions (500 μg L^{-1}) were prepared in methanol and stored in Tarsons® polypropylene tubes at −20 °C. The chemicals used to extract PFAS from concrete were methanol (LC-MS grade, >99.9%, Fisher Chemical) and ammonia solution (NH_3, reagent grade, 28%; Scharlau). Other chemicals used during solid phase extraction included ammonium acetate (reagent grade, 98%, Sigma-Aldrich) and formic acid (99%, Acros Organics). Ultrapure deionized (DI) water (18 MΩ, Milli-Q®, Millipore) was used to prepare extraction solutions and standards.

PFAS leachability from intact contaminated concrete monoliths

A semi-dynamic tank leaching test (modified LEAF 1315) was undertaken on concrete samples to assess the leachability of selected PFAS (PFOS, PFOA, PFHxS and PFHxA) from intact contaminated concrete simulating saturated conditions. The PFAS-contaminated concrete cores were collected from a pad at an FTA in Australia, where the temperature ranges between 0 and 45 °C and the annual rainfall is approx. 700 mm. The PFAS contamination at the FTA resulted from AFFF use between 1983 and 2010.

The details of concrete samples and semi-dynamic tank leaching test (modified LEAF 1315) conditions are given in Table 1. Three PFAS-contaminated concrete cores were characterized for PFAS by collecting powdered samples at ∼20 mm depth intervals along the core using a 10 mm methanol-prewashed diamond drill bit[17] (ESI SI 8†). The concrete cores were cut into half along the length and then into 2 cm thick sections using a methanol-prewashed diamond-tipped dry masonry cutting blade to yield semicircular half-pucks (designated hereon as monoliths). The monoliths with relatively similar PFOS + PFHxS concentrations in different cores were selected as replicates for the LEAF study and referred to as low- ($n = 3$), intermediate- ($n = 4$), and high-concentration ($n = 2$) concrete monolith replicates (Table 2).

The modified LEAF 1315 experiment was conducted in 2 L polypropylene jars which were thrice pre-rinsed with methanol and DI water. The jars were filled with 1 L of DI water, into which the weighed monoliths were fully immersed and suspended using a 0.28 mm nylon filament hanging from the lid (Fig. 1). At each sampling time point over the course of the experiment (0.08, 1, 2, 7, 14, 28, 42, 49, 63 and 91 d) (Table 1), a leachate sample was collected from the water in the jar (leachate) and sequentially replaced with a fresh 1 L of DI water. The time intervals for the replacement of the water varied from 2 h to 28 d (Table 1) as per the modified LEAF 1315 protocols.

At leachate sampling time points, the monoliths were removed, and excess water was allowed to drain into the polypropylene jars for ∼5 min. The monoliths were then placed onto pre-weighed polypropylene disks, and the weights of the monoliths containing the imbibed water were recorded. The leachates in polypropylene jars were homogenized by shaking, and ∼20 mL of the sample was removed for the determination of pH and electrical conductivity (EC) using a Mettler Toledo Duo pH and EC meter. One hundred mL of the homogenized leachate at sampling time points was removed and stored in polypropylene centrifuge tubes at 4 °C until sample preparation and analysis for PFAS by liquid chromatography-tandem mass spectrometry (LC-MS/MS). The jars were rinsed thrice with methanol and DI water, and the rinsates were stored in darkness at 4 °C until sample

Table 1 Concrete monolith samples and semi-dynamic tank leaching test conditions

Parameters	Properties
Concrete cores	Three PFAS-contaminated concrete cores[a]: core 1 (core 10), core 3 (core 12), and core 4 (core 13)
Concrete monoliths	Three cores with 2–4 field replicates Low concentration (core 1 replicate 3; core 3 replicates 1 and 2) Intermediate concentration (core 1 replicates 1 and 2; core 3 replicate 3; core 4 replicate 3) High concentration (core 4 replicates 1 and 2)
Concrete monolith dimensions	2 cm thickness × 9 cm diameter; cut in half to provide at least 5 cm dimension in one of the directions of mass transfer
The surface area of the concrete monolith	~110 cm^2 (~64 cm^2 for top and bottom of the monolith combined; ~28.3 cm^2 along the half circumference and 18 cm^2 flat surface through the diameter)
Leachate volume	1 L of ultrapure deionised water was replaced at each time interval for sample collection; the liquid-to-area ratio (L/A) of the fully immersed concrete monolith was ~9 mL cm^{-2}
Temperature	25 °C
pH	Ambient
Time interval duration between each replacement of the water bath volume	0.08, 1, 1, 5, 7, 14, 14, 7, 14, 28
Leachate sample collection time intervals – cumulative since the start of the experiment	0.08, 1, 2, 7, 14, 28, 42, 49, 63 and 91 d

[a] The concrete core numbers in Williams *et al.*[17] (core 10, core 12 and core 13) were renumbered in this study as core 1, core 3 and core 4, respectively.

Table 2 Initial PFAS concentrations in the concrete core monoliths

Core no.	Replicate	PFHxA (μg kg^{-1})	PFOA (μg kg^{-1})	PFHxS (μg kg^{-1})	PFOS (μg kg^{-1})	PFHxS + PFOS (μg kg^{-1})
Core 3	R1	19	313	408	553	962[b]
Core 3	R2	26	273	390	673	1063[b]
Core 3	R3	39	42	155	511	666[a]
Core 1	R1	37	28	140	458	599[a]
Core 1	R2	39	32	155	475	629[a]
Core 1	R3	57	412	533	824	1357[b]
Core 4	R1	34	939	1013	1067	2081[c]
Core 4	R2	50	834	919	1137	2056[c]
Core 4	R3	76	309	611	778	1390[b]

[a] Low concentration. [b] Intermediate concentration. [c] High concentration.

preparation and PFAS analysis by LC-MS/MS.[17,29] The polypropylene jars were then filled with fresh 1 L DI water and the monoliths were immersed again into the water and suspended until the subsequent sampling time point.

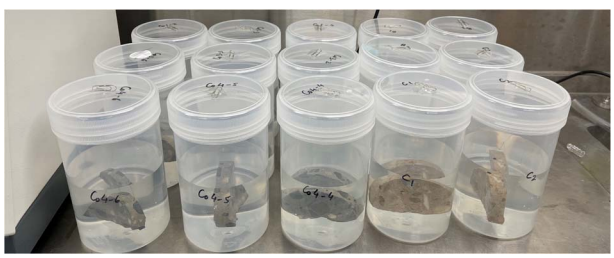

Fig. 1 Experimental setup for LEAF 1315 with concrete monoliths suspended in DI water.

After 91 d, concrete monoliths were removed, freeze-dried and ground to <2 mm particle size powder in a Rocklabs® Ring Mill pre-cleaned with methanol. The concrete powders were extracted using an alkaline methanol (methanol + 0.1% NH_3 solution) method and analyzed for PFAS using LC-MS/MS.[17,29] Calculations of total PFAS in concrete monoliths (μg kg^{-1}), the proportion of PFAS leached at sampling time points (%), cumulative mass (μg) and proportion (%) leached, and rate of PFAS leached (% d^{-1}) are given in the ESI (SI 1†).

Effect of pH on PFAS leachability from powdered concrete

A modified LEAF 1313 study was undertaken to investigate the leachability of PFAS from powdered (<2 mm) concrete at or near equilibrium pH conditions (ESI – SI 3†) at pH 7, 9, and 11 (temperature = 25 °C). A PFAS-contaminated concrete monolith

was freeze-dried and powdered to <2 mm particle size in a Rocklabs Ring Mill pre-cleaned with methanol.

Approximately 4 g of <2 mm powdered concrete samples were weighed into pre-weighed 50 mL polypropylene centrifuge tubes, to which 40 mL of pH 7, 9, or 11 DI water was added (adjusted using the required volume of 4 M HNO_3 determined through potentiometric titration) (ESI – SI 3†). The final powdered concrete to liquid (water) ratio was 1 : 10 (m/v). The suspensions were vortex-mixed for 30 s and, subsequently, gently agitated on an orbital shaker for 6 d. The pH and EC of the suspensions were recorded daily after the initial 3 d of agitation using a Mettler Toledo Duo pH and EC meter.

After 6 d, suspensions were centrifuged at 6120*g* for 20 min at 10 °C using a Beckman Coulter Avanti JXN-26 centrifuge. The supernatants were decanted into 50 mL polypropylene tubes, and the solid residues were weighed to record the imbibed leachate volumes. Samples (leachate and solids) were stored in darkness at 4 °C until preparation, extraction, and PFAS analysis by LC-MS/MS.[17,29]

Effect of particle size, duration of exposure to water and temperature on PFAS leachability from powdered concrete

An ASLP test was undertaken to examine the effect of particle size, duration of exposure to water and temperature on PFAS leachability from powdered concrete. Portions of contaminated concrete cores were crushed using an iron mortar and pestle pre-cleaned thrice with methanol and DI water, and sieved into three particle size fractions (*i.e.*, <2 mm, 2–20 mm and >20 mm).

To examine the effect of particle size, 2 g of <2 mm concrete powder, 10 g of 2–20 mm concrete solids, and 50 g of >20 mm concrete solids were weighed into 50 mL, 250 mL and 2 L polypropylene tubes, containers or jars, respectively, and into which 40 mL, 200 mL and 1 L of DI water were added (1 : 20 m/v). The polypropylene tubes, containers or jars were then placed on an end-over-end shaker for 24 h at 25 °C. Supernatants were decanted and solid residues were weighed to record the imbibed leachates. Solid residues were freeze-dried with the 2–20 mm and >20 mm size fraction samples ground into <2 mm powders using a Rocklabs® Ring Mill pre-cleaned with methanol.

To examine the effect of duration of exposure to water (0.5, 1, 2, 4, 8, 24, and 48 h), 2 g of <2 mm powdered concrete was weighed into 50 mL polypropylene centrifuge tubes, into which 40 mL of DI water was added (1 : 20 m/v). The suspensions were vortex-mixed for 30 s and then placed on an end-over-end shaker for a specific period (0–48 h) at 25 °C. At the completion of the shaking period, the suspensions were centrifuged at 6120*g* for 20 min at 10 °C using a Beckman Coulter Avanti JXN-26 centrifuge. The supernatants were decanted into 50 mL polypropylene tubes, and the solid residues were weighed to record the imbibed leachate.

To examine the effect of temperature (25 °C and 50 °C), 2 g of <2 mm powdered concrete was weighed into 50 mL polypropylene centrifuge tubes, into which 40 mL of DI water was added (1 : 20 m/v). The suspensions were vortex-mixed for 30 s and then placed on a temperature-controlled orbital shaker for 24 h at 25 °C and 50 °C, respectively. At the completion of the shaking period, the suspensions were centrifuged at 6120*g* for 20 min at 10 °C using a Beckman Coulter Avanti JXN-26 centrifuge. The supernatants were decanted into 50 mL polypropylene tubes, and the solid residues were weighed to record the imbibed leachate. The leachates and solid residues were prepared, extracted and analyzed for PFAS by LC-MS/MS as described previously by Srivastava *et al.*[29] and Williams *et al.*[17]

Leachate solid phase extraction and PFAS analysis by LC-MS/MS

Solid phase extraction (SPE) (clean-up and preconcentration) of leachate samples was conducted using 3 mL Phenomenex Strata™-X-AW cartridges.[17,29] Leachate samples (5 mL) were diluted 5 times with DI water to achieve pH ~ 6–7 to ensure PFAS adsorption onto the SPE cartridges. Fifty μL of a mixed internal standard with 5 ng of individual isotopically labelled PFAS (PFOS, PFOA, PFHxS and PFHxA) was added into the 25 mL diluted samples prior to SPE. The samples were loaded onto cartridges and eluted using an SPE vacuum manifold. The SPE cartridges were washed with 1 mL of 25 mM ammonium acetate (pH 6–7) followed by 1 mL of methanol. The PFAS were eluted from SPE cartridges using 0.5 mL of 5% formic acid in methanol into 2 mL polypropylene LC vials. The samples were diluted with 0.5 mL DI water (final volume = 1 mL), vortex-mixed for 30 s, and analyzed for PFAS by LC-MS/MS.[17,29] The limits of quantitation (LOQ) for PFAS in leachates/solution and solids are given in ESI SI 2.†

Residual powder extraction and PFAS analysis by LC-MS/MS

Approximately 0.5 g of <2 mm concrete powder was weighed in 50 mL polypropylene centrifuge tubes into which 50 μL of methanol-based internal standard mixture containing 5 ng of individual isotopically labelled PFAS (PFOS, PFOA, PFHxS and PFHxA) was added and vortex mixed for 30 s. After vortex mixing, 6 mL of methanol + 0.1% ammonia extraction solution was added, and the tube was placed in a SONICLEAN™ ultra-sonication bath at 25 °C for 20 min. The suspensions were then centrifuged at 6120*g* for 20 min at 10 °C using a Beckman Coulter Avanti JXN-26 centrifuge. The supernatants were then decanted into individual 50 mL polypropylene tubes. The solid residues were extracted twice again using 4 mL of methanol + 0.1% ammonia extraction solution, vortex-mixed for 30 s and placed in an ultra-sonication bath at 25 °C for 20 min. The suspensions were centrifuged, and supernatants removed. The three supernatants for individual samples were pooled for analysis (total volume = 16 mL). An aliquot of the pooled solution was analyzed for PFAS (PFOS, PFOA, PFHxS and PFHxA) concentrations using LC-MS/MS.[17,29]

Results and discussion

PFAS leachability from intact contaminated concrete monoliths

PFAS concentration in leachate. The pH of leachates during modified LEAF 1315 ranged between 9.6 and 11.7 (mean 11), whereas the EC ranged between 51 μS cm^{-1} and 763 μS cm^{-1}

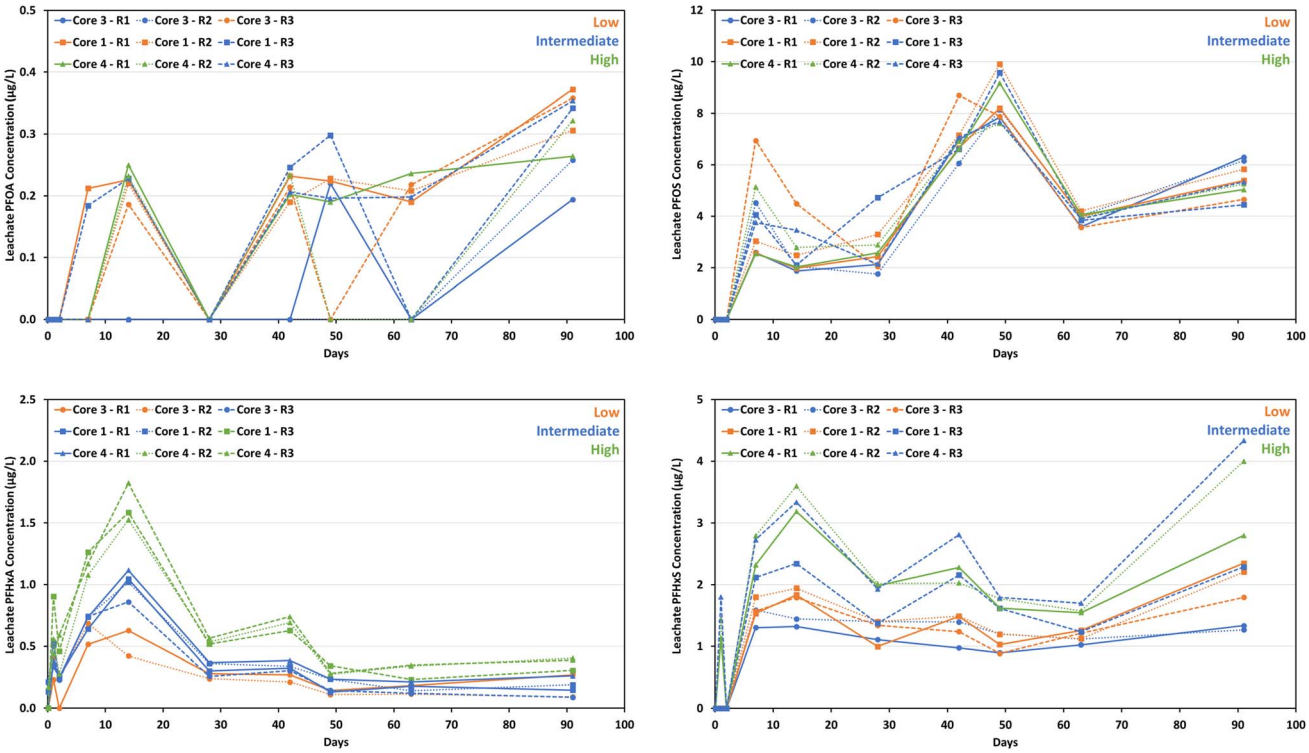

Fig. 2 PFAS concentrations (µg L^{-1}) in leachates at each sampling time point (d). The *x*-axis is the cumulative time across all time intervals.

(mean 308 µS cm^{-1}) (ESI – SI 4†). The EC of leachates initially increased with time and then declined over time (ESI – SI 4†).

PFOS, PFHxS, PFOA, and PFHxA concentrations leached from concrete monoliths at individual time points are presented in Fig. 2. In general, PFOS and PFHxS showed a similar leaching behavior regardless of the initial monolith concentrations (*i.e.*, low, intermediate, or high) (Fig. 2). For sampling time points ≤ 2 d, PFOS and PFHxS concentrations in leachates were <LOQ. At 7 to 91 d, the PFOS concentrations ranged from 1.8 to 9.9 µg L^{-1}, with most monoliths exhibiting two peaks at 7 and 49 d. Similarly, PFHxS concentrations ranged from 0.9 to 4.3 µg L^{-1} during this period, with two peaks observed at 14 and 42 d for most monoliths.

The leaching behavior of PFOA from concrete monoliths was variable across different sampling time points, ranging from <LOQ to 0.37 µg L^{-1} (Fig. 2). The consistently low PFOA concentrations (often <LOQ) compared to other PFAS examined indicated a stronger affinity of PFOA to the concrete matrix.

Contrarily, the leaching behavior of PFHxA from concrete monoliths differed from other PFAS examined (Fig. 2). In general, a similar leaching trend was observed regardless of the initial monolith concentrations. For sampling time points < 2 d, a rapid release of PFHxA was observed for all concrete monoliths. At 7 to 91 d, PFHxA concentrations leached from monoliths ranged from 0.1 to 1.8 µg L^{-1}. Leachable PFHxA concentrations peaked at 14 d, decreased to 28 d with a small increase at 42 d, and then decreased and remained constant until 91 d (Fig. 2). It implied that PFHxA was relatively highly leachable from the monoliths, in comparison to other PFAS reported here.

Proportion of PFAS leached. The proportions of PFOS, PFOA, PFHxS, and PFHxA leached from the concrete monoliths at different sampling time points and cumulatively are presented in Fig. 3 and 4. In general, the cumulative proportion of PFAS leached from the concrete monoliths decreased in the following order: PFHxA (>95%) > PFOS (26–84%) ≈ PFHxS (14–78%) > PFOA (<1–54%).

At ≤2 d, no PFOS leached above LOQ from the concrete monoliths (Fig. 3). The proportion of PFOS leached at individual sampling time points at >2 d ranged from 2% to 20% (Fig. 3). After 91 d, the cumulative proportion of PFOS leached ranged from 26% (core 4 R1 and R2 with high PFOS concentrations) to 84% (core 3 R1 with one of the lowest PFOS concentrations) (Fig. 4). Three concrete monoliths with low PFOS concentrations cumulatively leached 70–84% of their PFOS mass after 91 d. In general, the cumulative proportion of PFOS leached followed the order: low > intermediate > high concentration (Fig. 4).

Similar trends were observed for PFOA and PFHxS. After 91 d, low-concentration concrete monoliths cumulatively leached 26–54% of their PFOA mass, substantially higher than intermediate (1–4%) and high (<1%) concentration monoliths. The proportion of PFOA leached from the concrete monoliths at different sampling time points ranged from <1% to 14% (Fig. 3). Whereas the proportion of PFHxS leached from concrete monoliths at different sampling time points ranged between 1.4% and 18% (Fig. 3). Cumulatively, 69–78% of PFHxS mass

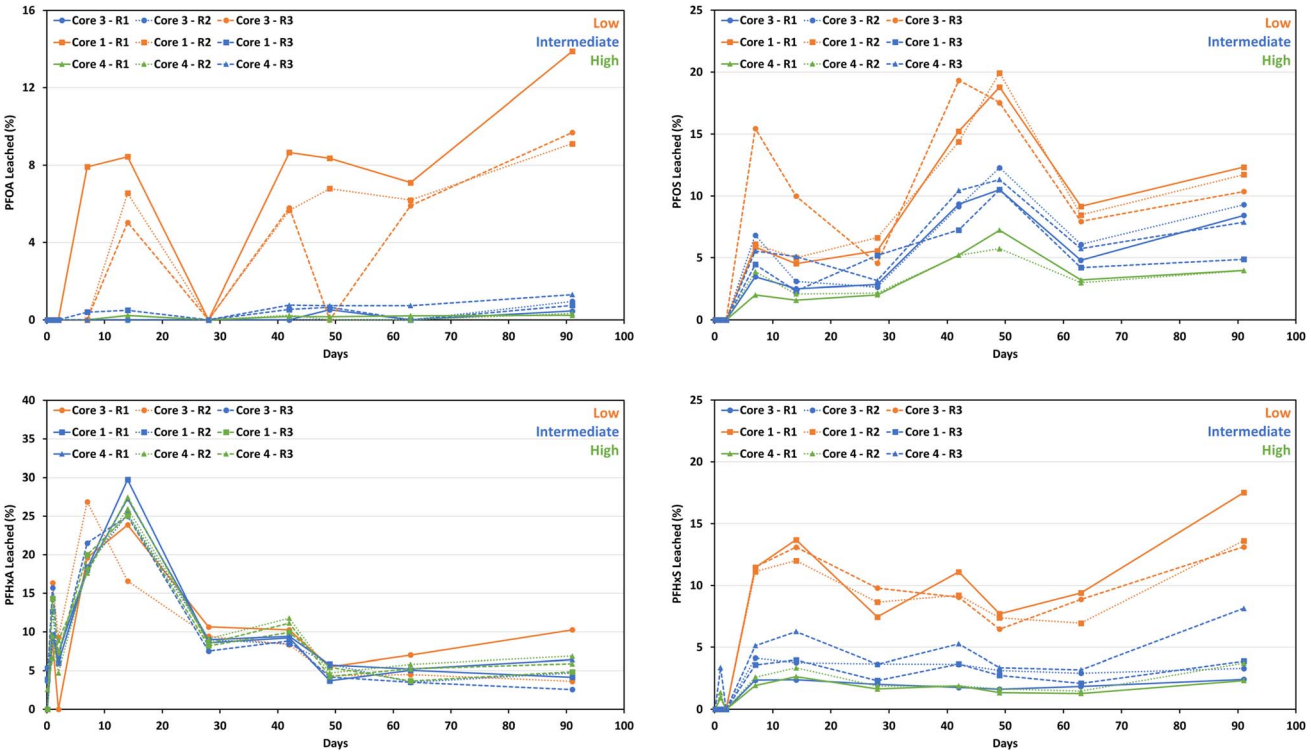

Fig. 3 Proportion of PFAS (%) leached from concrete monoliths at each sampling time point (d). The *x*-axis is the cumulative time across all time intervals.

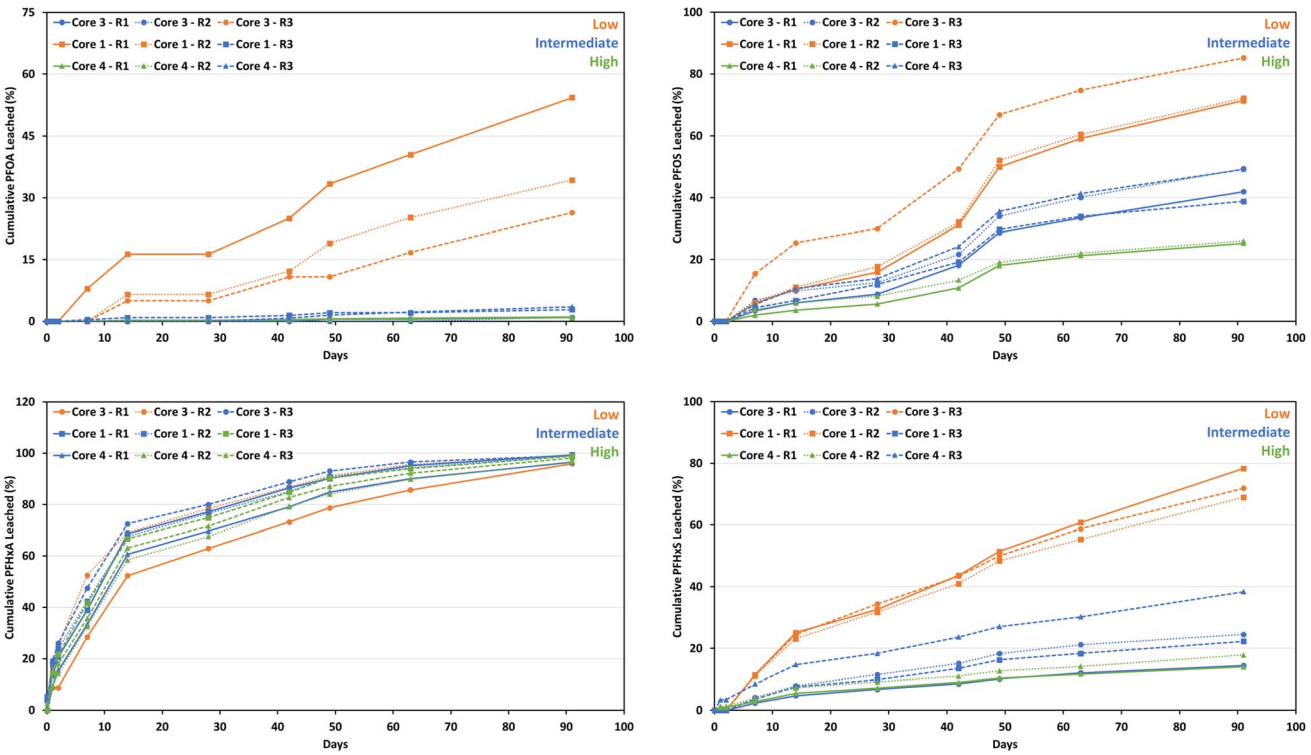

Fig. 4 Cumulative proportion of PFOS (%) leached from concrete monoliths at each sampling time point (d). The *x*-axis is the cumulative time across all time intervals.

was leached from low-concentration concrete monoliths, compared to intermediate- (22–38%) and high-concentration (14–18%).

In contrast, PFHxA exhibited a different behavior, as irrespective of the initial concentration, >95% of the total PFHxA mass leached from all monoliths after 91 d (Fig. 4). The proportion of PFHxA leached ranged from 2.5 to 30% (Fig. 3).

Rate of PFAS leachability. The rates of leachability for the long-chain PFAS (PFOS, PFOA, and PFHxS) over the sampling intervals showed similar trends (Fig. 5). Their leaching rates, indicated by the mean rate across sampling intervals (mean M-SI), attained maxima at intervals of 5–7 d (PFOS: 1.14% d^{-1}, PFOA: 0.18–0.30% d^{-1}, PFHxS: 1.16% d^{-1}) and then decreased at longer intervals such as at 14 and 28 d. The leaching rates also followed a consistent order based on the PFAS concentration in concrete (mean M-C), with low concentration exhibiting the highest rates, followed by intermediate and high concentrations. For PFOS, the rates were 0.80, 0.46, and 0.27% d^{-1} for low-, intermediate-, and high-concentration concrete monoliths, respectively. Whereas, for PFOA, the rates were 0.35%, 0.02%, and 0.01% for low-, intermediate-, and high-concentration concrete monoliths, respectively. Similarly, for PFHxS, the rates decreased from 0.76% d^{-1} (low) to 0.35% d^{-1} (intermediate) and 0.28% d^{-1} (high). We note that a larger variation in the leaching rate might be expected at 7 d, since the first 7 d duration was after 14 d of cumulative leaching, but the second 7 d duration was after 49 d of cumulative leaching (Table 1). This seems particularly evident for PFOA and PFHxS for the low-concentration cores.

The short-chain PFHxA displayed a contrasting behavior with a rapid initial release at ≤2 d, with the highest leaching rate of 16.9% d^{-1} observed at the 2 h interval. The leaching rate then gradually decreased with longer intervals, reaching 0.21% d^{-1} at 28 d. Unlike the long-chain PFAS, the leaching rate order based on PFHxA concentration was intermediate (6.93% d^{-1}) > high (3.89% d^{-1}) > low (2.86% d^{-1}). While the long-chain PFAS exhibited maximum leaching rates at intervals of 5–7 d and followed a consistent order based on PFAS monolith concentration, the short-chain PFHxA displayed a rapid initial release with a contrasting leaching rate order influenced by the initial monolith concentration.

PFAS leaching behavior from concrete. The behavior of PFAS in solids such as soils and sediments has been well documented in the literature.[30–32] Desorption of PFAS from solids has been reported to increase in the following order: carboxylic acids > sulfonic acids > sulfonamide functional groups, for the same C–F chain length.[31–35]

In our study, PFOA appears to be more strongly adsorbed onto concrete mineral phases than other PFAS, as the proportion of PFAS leached from concrete monoliths generally decreased in the following order: PFHxA > PFOS ≈ PFHxS > PFOA. Higher PFHxA leachability from concrete is consistent with previous findings for solids, whereas the lower leachability as compared to PFOS is inconsistent with most studies on solids, although similar observations have also been reported. Our findings suggest that PFOA is more strongly adsorbed on concrete mineral phases or retained within concrete pores than the other PFAS studied. Kabiri *et al.*[34] found relatively lower leaching of PFOA in comparison to PFOS from soils in a multiple extraction procedure. Gao and Chorover[36] reported that PFOA formed inner-sphere Fe-carboxylate complexes *via* ligand exchange (stronger bonds closer to surfaces), whereas PFOS formed outer-sphere complexes and hydrogen bonds (weaker bonds at a greater distance from the surface) at a hematite mineral surface. Hematite is likely to be present in concrete admixtures, leading to a similar mechanism

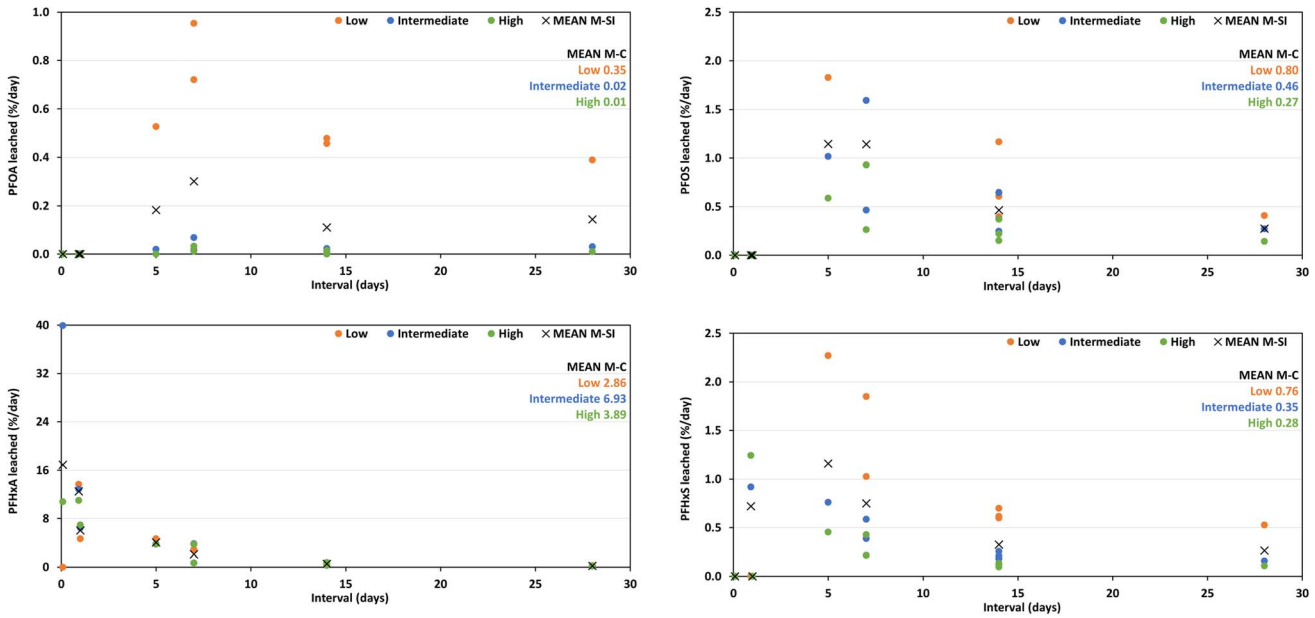

Fig. 5 The rate of PFAS leached (% d^{-1}) from concrete monoliths at different sampling intervals. Mean M-SI represents the mean of the rate of PFAS leachability from concrete monoliths for three concentration levels at a given sampling interval. Mean M-C represents the mean of the rate of PFAS leachability for each concentration level of concrete monolith regardless of the sampling interval.

responsible for decreased leaching of PFOA from concrete, as PFOA may form much stronger inner-sphere complexes between carboxylates and minerals present in concrete.

The partitioning of PFAS in macro- and micro-pores of cement/concrete could play an important role in leaching behavior. The porosity of concrete consists of air voids, capillary pores, and gel pores (or micropores).[37] Pore diameter distribution of a concrete monolith conducted through X-ray micro-computed tomography (CT) revealed that micropores (52 to <156 μm) and macropores (156 to 2444 μm) constituted 14–30% and 70–86%, respectively of the total porosity (ESI – SI 5†). It would be expected that prior to submerging the monoliths in water, the pores would be filled with air. Upon immersion into water, the air-filled voids would be expected to gradually be filled with water. In low-concentration concrete, PFAS may adsorb to readily available adsorption sites in macropores, which are larger and more accessible and have relatively lower specific surface area as compared to micropores. In high-concentration concrete, PFAS may have diffused further into micropores. Furthermore, the moisture status of the concrete may create variable air–water interfaces that influence PFAS leachability from micropores and macropores. A comprehensive analysis of the concrete's pore structure and the subsequent sequestration of PFAS within these pores linked to PFAS exchange processes at interfaces[38] is necessary for validation. Baduel *et al.*[14] estimated an 82 year period for 90% PFOS desorption from a concrete pad at an FTA with mean and maximum PFOS concentrations of 33 426 μg kg^{-1} and 223 983 μg kg^{-1}, respectively. Despite significantly higher PFOS concentrations in their study compared to ours (458–1137 μg kg^{-1}), both investigations demonstrated that high-concentration concrete exhibited lower PFAS leaching proportions, resulting in prolonged leaching durations. It is noteworthy that methodological differences exist between the studies, as Baduel *et al.*[14] employed wash-off leaching kinetics, whereas our study utilized the LEAF 1315 protocol under saturated conditions.

In contrast, the short-chain PFHxA displayed a rapid initial release within the first 2 d, with the highest leaching rate observed at the 2 h interval (Fig. 5). The leaching rate of PFHxA then gradually decreased with longer intervals, with earlier rates being high such that 50–70% of the PFAS mass is largely depleted within the first five leaching events (after a cumulative period of 14 d). Additionally, the order of leaching rates based on initial concentration (mean M-C) is also distinct for PFHxA. Here, the intermediate-concentration monolith exhibited the highest rate, followed by high and then low-concentration monoliths (Fig. 5). This contrasting behavior of PFHxA compared to long-chain PFAS suggested a potential influence of both pore-space partitioning and the initial PFAS concentration on the release mechanisms. The higher initial release from intermediate-concentration monoliths compared to other concentration monoliths requires further investigation.

Concrete is a mixture of cement minerals (*e.g.*, limestone, gypsum, and oxides/silicates, *e.g.*, belite ($2CaO \cdot SiO_2$), alite ($3CaO \cdot SiO_2$), Celite ($3CaO \cdot Al_2O_3$) and/or brownmillerite ($4CaO \cdot Al_2O_3 \cdot Fe_2O_3$)), sand, and small to large aggregates.[39] The aggregates, which can constitute approximately 70% of the concrete,[39] may include quartz, limestone, granite, and greenstone, all of which have the potential to be PFAS sorbents along with the cement, albeit with substantially less porosity and hence internal surface area than the co-existing cement phases. During and following concrete curing and diagenesis, a range of sometimes transient secondary mineral phases important to concrete structural integrity may also form.

In concrete, the potential drivers for adsorption and desorption in pores include but are not limited to, highly alkaline pH (*e.g.*, influencing PFAS and sorbent charges) and ionic strength (*e.g.*, competitive and bridging ions) conditions.[9] The pH of fresh concrete is strongly alkaline (~11), albeit decreasing over time with age/leaching, so PFOS, PFOA, PFHxS, and PFHxA ($pK_a < 3$) are expected to be present as deprotonated anions. Individual cement mineral surfaces (*e.g.*, portlandite, calcium silicates, aluminates, and hydroxides) and other solid phases in concrete, such as aggregate, have pH-dependent surface charges for electrostatic adsorption.[30,31] At pH 11, mineral phases in concrete are expected to have a negative surface charge (above their point of zero charge) and hence are expected to electrostatically repel anionic PFAS. Shih and Wang[40] found the adsorption of PFOS and PFOA on boehmite – sometimes found in soils – to decrease with an increase in pH, which was attributed to an increase in ligand exchange reactions and a decrease in electrostatic interaction. In the study by Campos-Pereira *et al.*,[41] the adsorption of PFAS (*e.g.*, C_3–C_5 and C_7–C_9 perfluorocarboxylates, C_4, C_6, and C_8 perfluorosulfonates, perfluorooctane sulfonamide, and 6 : 2 and 8 : 2 fluorotelomer sulfonates) onto ferrihydrite was found to be inversely related to pH, which was attributed to a decrease in solid surface ζ-potential with increasing pH.

Crucially, the extent of alkalinity and the suite of minerals present may alter substantially due to concrete aging. In particular, this aging process may involve the net loss of alkalinity and major cations *via* surface wicking or transport into underlying strata as a consequence of rainfall or fire-training activities.[42] Furthermore, the development of secondary minerals with the ability to alter the number and accessibility of internal pores may also influence PFAS leaching behavior. Anionic PFAS are likely to have electrostatic interactions with positively charged cations (*e.g.*, Ca^{2+} bridging or Al^{3+} network-forming) and/or undergo competitive exchange reactions with anions (*e.g.*, OH^-, CO_3^{2-}, HCO_3^-) in solution and/or solid phases in concrete.

Specifically, PFAS may have van der Waals interactions,[43] hydrogen bonds, or dipole–dipole interactions with the charged species[44] on concrete mineral surfaces. The strength of these interactions will depend on factors such as the chemical structure and size of the PFAS, as well as the charge and surface properties[45] of the concrete. The surfaces of concrete pores may also develop hydrophobic properties[46] due to impregnation of concrete with hydrophobic agents that could influence PFAS binding and retention through hydrophobic interactions. Other studies have also identified the potential for micelles formation in pores within sediments,[31] and this potential could also exist in concrete, given the internal porosity present. Accordingly,

further research is needed to elucidate the specific binding mechanism for PFAS (especially PFOA) under conditions present in concrete (pores) (*i.e.*, pH 11, high alkalinity, and elevated soluble calcium and aluminum concentrations).

The main mechanisms controlling water transport through concrete include wetting and drying cycles (and associated sorptivity and imbibition) and percolation of water through the available pore spaces.[47] The fraction of infiltrating water is likely to be small due to the low permeability of most concrete. Capillary action is expected to be the dominant water contact process at low permeability, and this includes water penetration due to capillary suction after the influence of capillary action on the evaporative drying of concrete.[48] In weathered concrete, percolation of water through cracks and/or pore networks may become a relatively more important water contact mechanism. However, in the current study, prominent cracks were avoided during sampling and evaporation is unlikely to be responsible for PFAS movement, as the concrete monoliths were fully submerged in water (*i.e.* LEAF 1315) or powdered concrete was equilibrated with water (*i.e.* ASLP or LEAF 1313) and PFAS could diffuse from concrete into the surrounding water.

Water soluble contaminants such as PFAS are likely transported into concrete pad pavements by water movement through pores driven by properties of the concrete (*e.g.*, permeability, pore space) leading to capillary imbibition and percolation if water saturations are high. Baduel *et al.*[14] found PFAS at depth (up to 12 cm) in an AFFF-contaminated concrete pad, and vertical transport was higher for short-chain PFAS. Recently, Williams *et al.*[17] reported the spatial and vertical (up to 20 cm depth) distribution of PFAS on/in a concrete fire training pad that had historical use of Ansulite and Lightwater AFFF. Individual PFAS were found to be more strongly associated with the cement fraction in concrete, which suggests the primary pathway for the transport of PFAS in concrete may be *via* the cemented porous portions of the media.[17]

Relationship between PFAS leachability and monolith mass. Despite efforts to standardize the size of concrete monoliths (half-pucks) used in this study, variations in initial dry mass occurred, ranging from 87 g to 135 g (mean = 106 g). The relationship between monolith mass and cumulative proportion of PFAS leached is presented in the ESI – SI 6.† In general, the cumulative proportion of PFAS leached from concrete monoliths decreased with increasing mass. A poor relationship between the proportion of PFAS leached and monolith mass may be due to several reasons. Firstly, the observed mass variation of monoliths might be relatively small compared to the inherent heterogeneity of PFAS aggregate, microfracture, and porosity distribution within the concrete monoliths.

Substantial variability in PFAS distribution within concrete was observed in this and previous studies.[14,17] Secondly, the surface area to volume ratio and density of the monoliths could be a more critical factor in governing PFAS leaching than monolith mass, as the proportion of aggregate relative to sand and cement could affect net porosity. Moreover, as the concrete monolith size and mass increase, the external surface area to volume ratio is expected to decrease. Accordingly, further investigations into the effect of monolith surface area to volume ratio and PFAS leaching behavior are warranted. Thirdly, factors including concrete microstructures such as porosity and pore size distribution might also influence leaching behavior by affecting the accessibility of water to PFAS within the concrete matrix.

Effect of pH on PFAS leachability from powdered concrete

After the addition of 4 M HNO_3, the initial pH of the concrete suspension was ~2 for pH 7 and 9 treatments, and ~8 for pH 11 treatment (ESI SI 7†). After 3 d, pH 11 concrete suspensions achieved the desired pH conditions and remained constant for the remainder of the study. For pH 9 and 7 concrete suspensions, the desired pH conditions for the study were not reached until 6 d. The EC of the concrete suspensions at pH 9 and 7 decreased at 3 d and then remained constant for the remainder of the study (ESI SI 7†). For pH 11, the EC of suspensions remained constant for the study period (ESI SI 7†).

The effect of pH (7, 9, and 11) on the leachability of PFOS, PFOA, PFHxS, and PFHxA from powdered concrete (<2 mm) investigated using a modified LEAF 1313 (Fig. 6a) demonstrated a significantly ($p < 0.05$) higher proportion of PFAS leached (88–91%) at pH 11 compared to pH 9 (51–69%) and pH 7 (60–71%). A decrease in PFAS leachability with decreasing pH may be attributed to changes in surface charge and solubility of some hydroxide or carbonate mineral phases in the concrete leading to net PFAS release from previously occluded pores or microfracture. As mentioned previously cement mineral surfaces and aggregates, will likely have pH-dependent surface charges for electrostatic adsorption[30,31] with negative surface charges at pH 11 and decreasing negative surface charges with a decrease in pH. The reduction in negative surface charge with pH leads to reduced electrostatic repulsion between the concrete surface and anionic PFAS.[40] In addition, the solubility of concrete solid phases due to changes in pH will likely influence PFAS binding and leachability due to weak electrostatic interactions with released positively charged cations.

Effect of particle size, duration of exposure to water and temperature on PFAS leachability from concrete powder

The effect of concrete particle size (Fig. 6b), duration of exposure to water (Fig. 6c), and temperature (Fig. 6d) on PFOS, PFOA, PFHxS, and PFHxA leachability was investigated using ASLP. A significantly higher proportion of PFAS leachability of ($p < 0.05$) was observed in the <2 mm concrete powder (mean 95–99%) as compared to 2–20 mm (mean 3–79%) and >20 mm (mean 3–66%) size fractions (Fig. 6b). The proportion of PFOS leached was significantly lower ($p < 0.05$) in the >20 mm (mean = 40%) size fraction compared to the 2–20 mm (mean = 62%) size fraction. No significant difference ($p > 0.05$) in the proportion of PFOA, PFHxS, and PFHxA leachability was found between the 2–20 mm and >20 mm size fractions (Fig. 6b).

A higher PFAS leachability with decreasing concrete particle size could be attributed to an increase in surface area and access of the water (solvent) to solid interfaces in concrete pores. Pang *et al.*[49] found increased PFAS water leachability from soil using a gas fractionation-enhanced technology when ground to a fine

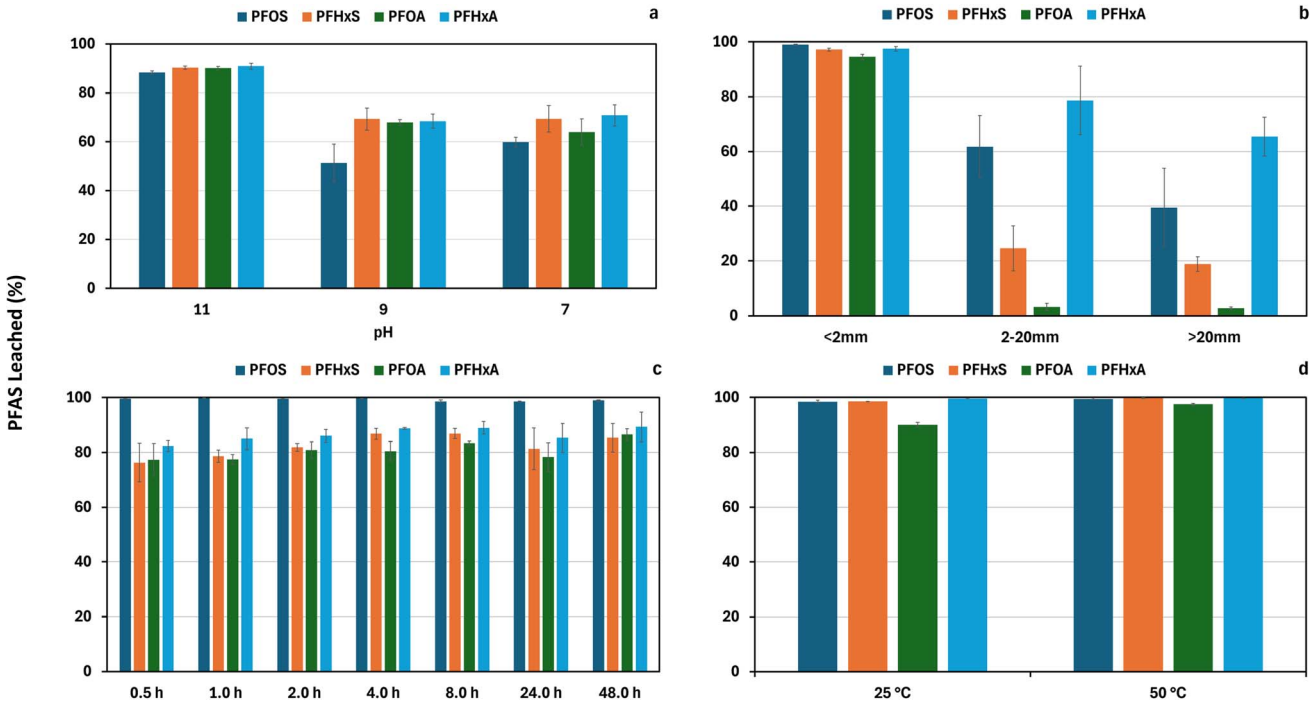

Fig. 6 Effect of (a) pH, (b) particle size, (c) duration of exposure to water and (d) temperature on PFAS leachability from concrete powder.

powder. The authors attributed the increased PFAS extraction to the finer soil particles having greater specific surface areas and access to PFAS adsorbed within pores. The particle size reduction of concrete (comminution) is likely to have resulted in fundamental changes in concrete morphology.[50] These morphological changes could include the generation of powders from larger >2 mm aggregates present in cement such as angular clasts, anhydrous cement phases, and oxides (*e.g.*, $CaO{\cdot}Al_2O_3$ and $CaO{\cdot}Al_2O_3{\cdot}Fe_2O_3$). This particle size reduction and changes in morphological changes of cement would have increased the solid surface area and generated a suite of new mineral sizes, surface and edge morphologies, microfractures, and detached cement phases from sand and aggregate.[51]

In this study, duration of exposure to water (0.5–48 h) and temperature (25 °C and 50 °C) were found to have little observable influence on the proportion of PFAS leached from powdered concrete (Fig. 6c and d). The absence of an influence for these parameters could be due to the already observed high leachability of PFAS (>75%) in water from the powdered concrete used in ASLP. In a contaminated soil washing study, Pang *et al.*[49] found PFAS leaching to decrease by >5% with an increased equilibration period from 5 min to 4 d (the greatest decrease of 38% was observed for PFOS). The authors suggested the decrease in PFAS concentrations in water with duration of exposure to water was likely due to clay swelling and interlayer anion adsorption.[49] Considering the potential for similar PFAS leaching behavior in concrete and soils, further research is warranted to investigate the long-term leaching dynamics of PFAS from concrete under various environmental conditions.

PFAS concrete management

Common leaching tests, *viz.*, LEAF 1313 and 1315 and ASLP, were used in this study to evaluate PFAS leachability from concrete. These tests have been applied broadly to inorganic and organic contaminants in a range of soil and solid matrices, although these standard tests were primarily developed for inorganic contaminants and soil matrices. Further research is needed to assess the usefulness of the standard tests and approaches to assess PFAS leachability from concrete, and if required, develop new or adapt existing leaching tests that can be validated under field conditions. Modeling is also needed to integrate processes at the scales that influence PFAS partitioning to interfaces and surfaces within concrete.[38]

Future standard tests for PFAS leachability from concrete should consider the incorporation of monolith and pore surface area and how findings can be applied to different management options, for example, in-place concrete pad wash-off, stockpiles, reuse scenarios such as in road base, and landfill disposal. In representing the release of PFAS from concrete under field conditions, possible limitations of the LEAF method are the use of water-saturated conditions surrounding the monolith rather than just the exposed surface as with a pad, the lack of wet–dry cycles that might be experienced in the field, the prolonged exposure time in the LEAF testing of up to 28 days at a time compared to episodic and shorter term water applications to pads *via* rainfall events of pad use, and possibly biased outcomes due to the small scale (5–10 cm length scales) of recovered monolith samples compared to the concrete pad scale of 10 s of meters. To address a number of these potential limitations for pads, there is scope to evaluate field-wash-off

testing of portions or the whole of PFAS-impacted pads as a method to gain confidence in laboratory LEAF outcomes in representing field pad responses. Such testing would provide averaging over larger areas of PFAS variability, allow sequential wet–dry cycling, and controlled periods of water exposure.

The high leachability of PFAS, especially PFOS, PFHxA, and PFHxS, observed from concrete in this study highlights the importance of correctly managing these materials (*in situ* and *ex situ*) at sites to ensure they are not a continuing source of contamination into the environment. The finding that PFAS leachability in water from concrete increases with decreasing particle size suggests that a phased physical separation process may be a feasible management option to reduce the PFAS load (on- or off-site) in concrete. When demolishing concrete, larger aggregates with lower PFAS concentrations could be physically separated from crushed concrete with smaller particle sizes. The remaining predominantly cementitious material could be further crushed to a <2 mm powder, water leached (or *via* flotation), and concentrated on a sorbent material as previously demonstrated for soils (*i.e.*, soil washing).[52,53] The leachates could be preconcentrated onto a sorbent material for disposal or treatment using destructive technology. Alternatively, Douglas *et al.*[18] suggested that PFAS-contaminated concrete could be successfully managed in the short term *in situ* through the application of sealants that prevent water penetration and PFAS leachability. Standard concrete sealants could be enhanced through the addition of sorbent materials or advanced materials that bind PFAS (*e.g.*, powdered activated carbon).

Conclusions

This study shed light on the complexities of PFAS leaching from concrete, highlighting the interplay between specific PFAS characteristics (*e.g.*, chain length, functional groups and concentration range) and concrete properties (*e.g.*, pH, porosity, mineralogy). PFAS leachability from intact concrete monoliths varied significantly depending on the PFAS type, as PFOA exhibited a lower leachability compared to other PFAS tested, suggesting a stronger binding affinity to concrete. Contrariwise, PFHxA was readily leached and depleted more rapidly from all concrete core samples than the other PFAS. These findings emphasize the importance of considering individual PFAS properties when assessing leaching risks. The study also revealed the influence of environmental factors on PFAS leaching. Decreasing the pH from the highly alkaline environment within concrete pores resulted in lower leachability, suggesting a potential role of surface charge interactions. Particle size also played a significant role, with smaller concrete fragments exhibiting higher leachability. This suggests that crushing concrete could be a strategy to enhance the effectiveness of treatment techniques like washing to remove PFAS. This study also highlighted gaps in our understanding of PFAS behavior in concrete. Current leaching protocols, designed for worst-case scenarios in soil over extended periods, may not accurately reflect leaching behavior in concrete under various naturally occurring or re-engineered (*e.g.*, in road base) environmental conditions. Furthermore, the specific binding mechanisms of PFAS within concrete's unique pore environment (high pH, presence of calcium and aluminum, aggregates, and cement) remain unclear. This knowledge gap limits the development of effective treatment technologies for PFAS-contaminated concrete. Future research should focus on addressing these identified gaps. Development of new or adapted leaching tests specifically designed for PFAS in concrete, validated under field conditions, is crucial. These tests should consider factors like real-world leaching rates and point-in-time concentration measurements. Additionally, research into the specific binding mechanisms of PFAS in concrete is essential for a more comprehensive understanding of leaching behavior and the development of targeted treatment strategies. Building upon the finding of increased leachability with decreasing particle size, exploring the feasibility of physical separation processes, potentially combined with chemical or destructive technologies, holds promise for future PFAS remediation approaches in concrete infrastructures.

Data availability

Data may be made available on request.

Author contributions

Prashant Srivastava: conceptualization, methodology, investigation, writing – original draft, project administration, funding acquisition; Grant Douglas: writing – review & editing, conceptualization; Greg B. Davis: writing – review & editing, conceptualization, funding acquisition; Rai S. Kookana: writing – review & editing, conceptualization, funding acquisition; Canh Tien Trinh Nguyen: investigation; Mike Williams: investigation, writing – review & editing; Karl Bowles: writing – review & editing, conceptualization; Jason K. Kirby: writing – review & editing, funding acquisition, conceptualization.

Conflicts of interest

There are no conflicts to declare.

Acknowledgements

This work was funded by the Australian Department of Defence. The authors acknowledge the Australian Department of Defence team particularly, Mr Garbis Avakian, Ms Nelma Akhund, Mr Stephen Corish, Mr Darren Skuse and Mr Mark Bauer, for their expert assistance in a number of aspects related to this study.

References

1 R. C. Buck, J. Franklin, U. Berger, J. M. Conder, I. T. Cousins, P. de Voogt, A. A. Jensen, K. Kannan, S. A. Mabury and S. P. van Leeuwen, Perfluoroalkyl and polyfluoroalkyl substances in the environment: terminology, classification, and origins, *Integr. Environ. Assess. Manage.*, 2011, **7**, 513–541.

2 M. Lorenzo, J. Campo and Y. Pico, Optimization and comparison of several extraction methods for determining perfluoroalkyl substances in abiotic environmental solid matrices using liquid chromatography-mass spectrometry, *Anal. Bioanal. Chem.*, 2015, **407**, 5767–5781.
3 S. Mejia-Avendano, G. Munoz, S. Sauve and J. X. Liu, Assessment of the Influence of Soil Characteristics and Hydrocarbon Fuel Cocontamination on the Solvent Extraction of Perfluoroalkyl and Polyfluoroalkyl Substances, *Anal. Chem.*, 2017, **89**, 2539–2546.
4 M. P. Krafft and J. G. Riess, Selected physicochemical aspects of poly- and perfluoroalkylated substances relevant to performance, environment and sustainability-Part one, *Chemosphere*, 2015, **129**, 4–19.
5 Australian Department of Defence, *Department of Defence Annual Report 2021–22*, 2022.
6 S. Balgooyen and C. K. Remucal, Impacts of Environmental and Engineered Processes on the PFAS Fingerprint of Fluorotelomer-Based AFFF, *Environ. Sci. Technol.*, 2023, **57**, 244–254.
7 A. Nickerson, A. C. Maizel, C. E. Schaefer, J. F. Ranville and C. P. Higgins, Effect of geochemical conditions on PFAS release from AFFF-impacted saturated soil columns, *Environ. Sci.: Processes Impacts*, 2023, **25**, 405–414.
8 Australian Department of Health, *Per- and Poly-Fluoroalkyl Substances (PFAS) Health Effects and Exposure Pathways*, 2022.
9 G. B. Douglas, J. L. Vanderzalm, M. Williams, J. K. Kirby, R. S. Kookana, T. P. Bastow, M. Bauer, K. C. Bowles, D. Skuse and G. B. Davis, PFAS contaminated asphalt and concrete – Knowledge gaps for future research and management, *Sci. Total Environ.*, 2023, **887**, 164025.
10 X. Lyu, F. Xiao, C. Shen, J. Chen, C. M. Park, Y. Sun, M. Flury and W. Dengjun, Per- and Polyfluoroalkyl Substances (PFAS) in Subsurface Environments: Occurrence, Fate, Transport, and Research Prospect, *Rev. Geophys.*, 2022, **60**, e2021RG000765.
11 B. Hubertus, A. Gottfried, K. Wolfgang, R. Gerd, S. Klaus Günter and V. Ingo, PFAS: forever chemicals—persistent, bioaccumulative and mobile. Reviewing the status and the need for their phase out and remediation of contaminated sites, *Environ. Sci. Eur.*, 2023, **35**, 1–50.
12 Z. Matthias, D. Julia, B. Alfred Paul, Z. Ottavia, L. E. Yangutov and O. Łukasz, Vienna, Austria, 2023.
13 L. Rainer and J. L. Robert, The universe of fluorinated polymers and polymeric substances and potential environmental impacts and concerns, *Curr. Opin. Green Sustainable Chem.*, 2023, **41**, 100795.
14 C. Baduel, C. J. Paxman and J. F. Mueller, Perfluoroalkyl substances in a firefighting training ground (FTG), distribution and potential future release, *J. Hazard. Mater.*, 2015, **296**, 46–53.
15 Y. Li, T. A. Key, P. H. N. Vo, S. Porman, A. Thapalia, J. T. McDonough, S. Fiorenza, C. M. Barnes, J. F. Mueller and P. K. Thai, Distribution and release of PFAS from AFFF-impacted asphalt: how does it compare to concrete?, *J. Hazard. Mater.*, 2024, **466**, 133627.
16 P. K. Thai, J. T. McDonough, T. A. Key, J. Thompson, P. Prasad, S. Porman and J. F. Mueller, Release of perfluoroalkyl substances from AFFF-impacted concrete in a firefighting training ground (FTG) under repeated rainfall simulations, *J. Hazard. Mater. Lett.*, 2022, **3**, 100050.
17 M. Williams, G. Douglas, J. Du, J. Kirby, R. Kookana, J. Pengelly, G. Watson, K. Bowles and G. Davis, Quantification of the variability and penetration of per- and poly-fluoroalkyl substances through a concrete pad, *Chemosphere*, 2023, **333**, 138903.
18 G. B. Douglas, J. L. Vanderzalm, J. K. Kirby, M. Williams, T. P. Bastow, M. Bauer, K. C. Bowles, D. Skuse, R. S. Kookana and G. B. Davis, Sealants and Other Management Strategies for PFAS-Contaminated Concrete and Asphalt, *Curr. Pollut. Rep.*, 2023, **9**, 603–622.
19 USEPA, *SW-846 Test Method 1313: Liquid-Solid Partitioning as a Function of Extract pH Using a Parallel Batch Extraction Procedure*, 2017.
20 USEPA, *SW-846 Test Method 1314: Liquid-Solid Partitioning as a Function of Liquid–Solid Ratio for Constituents in Solid Materials Using an Up-Flow Percolation Column Procedure*, 2017.
21 USEPA, *SW-846 Test Method 1315: Mass Transfer Rates of Constituents in Monolithic or Compacted Granular Materials Using a Semi-dynamic Tank Leaching Procedure*, 2017.
22 USEPA, *SW-846 Test Method 1316: Liquid-Solid Partitioning as a Function of Liquid-To-Solid Ratio in Solid Materials Using a Parallel Batch Procedure*, 2017.
23 Standards Australia, *Australian Standard Leaching Procedure (ASLP) Tests (Australian Standard AS4439) – Wastes, Sediments and Contaminated Soils Part 3: Preparation of Leachates — Bottle Leaching Procedure*, 1997.
24 Government of Western Australia, *Background Paper on the Use of Leaching Tests for Assessing the Disposal and Re-use of Waste-Derived Materials*, 2015.
25 HEPA, *Draft PFAS National Environmental Management Plan Version 3.0, Heads of EPAs Australia and New Zealand*, 2022.
26 D. A. Navarro, S. Kabiri, J. A. T. Ho, K. C. Bowles, G. Davis, M. J. McLaughlin and R. S. Kookana, Stabilisation of PFAS in soils: long-term effectiveness of carbon-based soil amendments, *Environ. Pollut.*, 2023, **323**, 121249.
27 J. L. Rayner, D. Slee, S. Falvey, R. Kookana, E. Bekele, G. Stevenson, A. Lee and G. B. Davis, Laboratory batch representation of PFAS leaching from aged field soils: intercomparison across new and standard approaches, *Sci. Total Environ.*, 2022, **838**, 156562.
28 M. Williams, G. Douglas, J. Du, J. Kirby, R. Kookana, G. Pengelly, G. Watson and G. B. Davis, Bandiana Military Area – PFAS in Fire Training Area Concrete, *CSIRO Australia Report for the Department of Defence (Confidential)*, CSIRO, Australia, 2023.
29 P. Srivastava, M. Williams, J. Du, D. Navarro, R. Kookana, G. Douglas, T. Bastow, G. Davis and J. K. Kirby, Method for extraction and analysis of per- and poly-fluoroalkyl substances in contaminated asphalt, *Anal. Methods*, 2022, **14**, 1678–1689.

30 M. G. Evich, M. J. B. Davis, J. P. McCord, B. Acrey, J. A. Awkerman, D. R. U. Knappe, A. B. Lindstrom, T. F. Speth, C. Tebes-Stevens, M. J. Strynar, Z. Y. Wang, E. J. Weber, W. M. Henderson and J. W. Washington, Per- and polyfluoroalkyl substances in the environment, *Science*, 2022, **375**, 512.

31 R. S. Kookana, D. A. Navarro, S. Kabiri and M. J. McLaughlin, Key properties governing sorption-desorption behaviour of poly- and perfluoroalkyl substances in saturated and unsaturated soils: a review, *Soil Res.*, 2023, **61**, 107–125.

32 T. M. H. Nguyen, J. Braunig, K. Thompson, J. Thompson, S. Kabiri, D. A. Navarro, R. S. Kookana, C. Grimison, C. M. Barnes, C. P. Higgins, M. J. McLaughlin and J. F. Mueller, Influences of Chemical Properties, Soil Properties, and Solution pH on Soil-Water Partitioning Coefficients of Per- and Polyfluoroalkyl Substances (PFASs), *Environ. Sci. Technol.*, 2020, **54**, 15883–15892.

33 C. P. Higgins and R. G. Luthy, Sorption of Perfluorinated Surfactants on Sediments, *Environ. Sci. Technol.*, 2006, **40**, 7251–7256.

34 S. Kabiri, W. Tucker, D. A. Navarro, J. Braunig, K. Thompson, E. R. Knight, T. M. H. Nguyen, C. Grimison, C. M. Barnes, C. P. Higgins, J. F. Mueller, R. S. Kookana and M. J. McLaughlin, Comparing the Leaching Behavior of Per- and Polyfluoroalkyl Substances from Contaminated Soils Using Static and Column Leaching Tests, *Environ. Sci. Technol.*, 2022, **56**, 368–378.

35 S. Rayne and K. Forest, Congener-specific organic carbon-normalized soil and sediment-water partitioning coefficients for the C1 through C8 perfluoroalkyl carboxylic and sulfonic acids, *J. Environ. Sci. Health, Part A: Toxic/Hazard. Subst. Environ. Eng.*, 2009, **44**, 1374–1387.

36 X. D. Gao and J. Chorover, Adsorption of perfluorooctanoic acid and perfluorooctanesulfonic acid to iron oxide surfaces as studied by flow-through ATR-FTIR spectroscopy, *Environ. Chem.*, 2012, **9**, 148–157.

37 C. Ruixing, M. Song and L. Jiaping, Relationship between chloride migration coefficient and pore structures of long-term water curing concrete, *Constr. Build. Mater.*, 2022, **341**, 127741.

38 K. Sookhak Lari, G. B. Davis, A. Kumar, J. L. Rayner, X.-Z. Kong and M. O. Saar, The Dynamics of Per- and Polyfluoroalkyl Substances (PFAS) at Interfaces in Porous Media: A Computational Roadmap from Nanoscale Molecular Dynamics Simulation to Macroscale Modeling, *ACS Omega*, 2024, **9**, 5193–5202.

39 Cement Concrete & Aggregates Australia, *A Guide to Concrete Construction 2020 — Part II-Section 1 — Cements*, 2020, pp. 1–21.

40 K. M. Shih and F. Wang, Adsorption behavior of perfluorochemicals (PFCs) on boehmite: influence of solution chemistry, *Procedia Environ. Sci.*, 2013, **18**, 106–113.

41 H. Campos-Pereira, J. Makselon, D. B. Kleja, I. Prater, I. Kogel-Knabner, L. Ahrens and J. P. Gustafsson, Binding of per- and polyfluoroalkyl substances (PFASs) by organic soil materials with different structural composition – charge- and concentration-dependent sorption behavior, *Chemosphere*, 2022, **297**, 9.

42 A. J. Boyd and J. P. Skalny, in *Environmental Deterioration of Materials*, ed. A. Moncmanová, WIT Press, Southampton, UK, 2007, ch. 5, vol. 28, pp. 143–184.

43 Y. X. Zhang, G. Cornelissen, L. Silvani, V. Zivanovic, A. B. Smebye, E. Sormo, G. Thune and G. Okkenhaug, Industrial byproducts for the soil stabilization of trace elements and per- and polyfluorinated alkyl substances (PFASs), *Sci. Total Environ.*, 2022, **820**, 11.

44 H. Li, Q. Dong, M. Zhang, T. Gong, R. Zan and W. Wang, Transport behavior difference and transport model of long- and short-chain per- and polyfluoroalkyl substances in underground environmental media: a review, *Environ. Pollut.*, 2023, **327**, 121579.

45 D. P. Oliver, Y. S. Li, R. Orr, P. Nelson, M. Barnes, M. J. McLaughlin and R. S. Kookana, The role of surface charge and pH changes in tropical soils on sorption behaviour of per- and polyfluoroalkyl substances (PFASs), *Sci. Total Environ.*, 2019, **673**, 197–206.

46 S. B. Atla, Y.-H. Huang, J. Yang, H.-J. Chen, Y.-H. Kuo, C.-M. Hsu, W.-C. Lee, C.-C. Chen, D.-W. Hsu and C.-Y. Chen, Hydrophobic Calcium Carbonate for Cement Surface, *Crystals*, 2017, **7**, 371.

47 X. Zhang and H. Zhao, Characterization of Moisture Diffusion in Cured Concrete Slabs at Early Ages, *Adv. Mater. Sci. Eng.*, 2015, **2015**, 154394.

48 C. Hall, Water Sorptivity of Mortars and Concretes – A Review, *Mag. Concr. Res.*, 1989, **41**, 51–61.

49 H. Pang, B. Dorian, L. Gao, Z. Xie, M. Cran, S. Muthukumaran, F. Sidiroglou, S. Gray and J. Zhang, Remediation of poly-and perfluoroalkyl substances (PFAS) contaminated soil using gas fractionation enhanced technology, *Sci. Total Environ.*, 2022, **827**, 154310.

50 P. C. C. Gomes, C. Ulsen, F. A. Pereira, M. Quattrone and S. C. Angulo, Comminution and sizing processes of concrete block waste as recycled aggregates, *Waste Manage.*, 2015, **45**, 171–179.

51 C. Ulsen, E. Tseng, S. C. Angulo, M. Landmann, R. Contessotto, J. T. Balbo and H. Kahn, Concrete aggregates properties crushed by jaw and impact secondary crushing, *J. Mater. Res. Technol.*, 2019, **8**, 494–502.

52 C. Grimison, E. R. Knight, T. M. H. Nguyen, N. Nagle, S. Kabiri, J. Braunig, D. A. Navarro, R. S. Kookana, C. P. Higgins, M. J. McLaughlin and J. F. Mueller, The efficacy of soil washing for the remediation of per- and poly-fluoroalkyl substances (PFASs) in the field, *J. Hazard. Mater.*, 2023, **445**, 8.

53 A. Hoisaeter, H. P. H. Arp, G. Slinde, H. Knutsen, S. E. Hale, G. D. Breedveld and M. C. Hansen, Excavated *vs.* novel *in situ* soil washing as a remediation strategy for sandy soils impacted with per- and polyfluoroalkyl substances from aqueous film forming foams, *Sci. Total Environ.*, 2021, **794**, 9.